Magnetic Stimulation of Curved Nerves

A. Rotem and E. Moses*

***Abstract*—Magnetic stimulation of nerves is attracting increased attention recently, as it has been found to be useful in therapy of neural disorders in humans. In an effort to explain the mechanisms of magnetic stimulation, we focus in this paper on the dependence of magnetic stimulation on neuronal morphology and in particular on the importance of curvature of axonal bundles. Using the theory of passive membrane dynamics, we predict the threshold power (the minimum stimulation power required to initiate an action potential) of specific axonal morphologies. In the experimental section, we show that magnetic stimulation of the frog sciatic nerve follows our theoretical predictions. Furthermore, the voltage length constant of the nerve can be measured based on these results alone.**

***Index Terms*—Curvature, magnetic stimulation, nerve, threshold power, voltage length constant.**

I. Introduction

SINCE the first transcranial magnetic stimulation (TMS) was conducted by Barker *et al.* [1] in 1985, it has become a remarkable tool for neuroscience research. As a painless means to probe into human brains, TMS continuously gains diagnostic and therapeutic applications [2]–[4]. Despite the impressive progress, there is a wide agreement that the full clinical potential of TMS, mainly as an alternative to electroconvulsive therapy (ECT) is still unrealized [5]–[7], with one of the main drawbacks being the incomplete comprehension of the physical mechanisms that underlie TMS. It is particularly not clear why certain regions in the brain are excitable while others are not, but brain geometry and the anatomy of sulci and gyri seem to play a role in this mechanism [8]–[12]. This fact motivates us to further explore how curvature modulates the effect of magnetic stimulation.

In this paper, we rely on measurements of the TMS threshold—i.e., the minimum TMS power required for stimulating an action potential. The TMS threshold is affected mainly by the passive properties of the nerve, a fact that both simplifies theoretical prediction and provides a technique for direct measurement of the voltage length constant of the axon. The length constant determines how far along the axon electric perturbations can propagate without the help of voltage gated channels, which actively revive the signal.

In healthy myelinated axons, the length constant is proportional to the distance between neighboring nodes of Ranvier (internodal length), thus enabling proper saltatory conduction of action potentials along the axon. Decrease in the length constant is an indicator for loss of insulation of the axon, possibly due to demyelination. Mismatches between the internodal length and the voltage length constant are considered one of the main causes for demyelinating diseases of the nervous system such as multiple sclerosis [13]. Determination of the length constant is, therefore, an interesting issue with practical implications of its own.

Manuscript received January 30, 2005; revised June 28, 2005. This work was supported in part by the Clore Foundation. *Asterisk indicates corresponding author.*

A. Rotem is with the Weizmann Institute of Science, PO Box 26, Rehovot 76100 Israel (e-mail: assaf.rotem@weizmann.ac.il).

*E. Moses is with the Weizmann Institute of Science, PO Box 26, Rehovot 76100 Israel (e-mail: elisha.moses@weizmann.ac.il).

Digital Object Identifier 10.1109/TBME.2005.869770

II. Theoretical Background

Subthreshold dynamics of the axonal membrane voltage are readily expressed by the passive conductance cable equation [14]

$$\lambda^2 \frac{\partial^2 V_m}{\partial x^2} - \tau \frac{\partial V_m}{\partial t} - V_m = \lambda^2 \frac{\partial E_x}{\partial x}. \tag{1}$$

Here, V_m is the axon membrane potential, λ is the length constant of the axon, τ is the time constant of the axon and x is directed along the axon, regardless of its true absolute orientation. E_x is the projection of the effective external electric field on the direction of the axon at any point along it.

Super-threshold (active membrane) dynamics are ignored here, under the assumption that an action potential is generated at any point x along the axon for which $V_m(x) = V_T$, where V_T is the threshold voltage of the axon. This simplification is justified for the type of experiment that we conducted, which measures the threshold stimulation value, i.e., the minimum current discharge inside the axon required for stimulating an action potential.

In the case of magnetic stimulation, the external electric field is the result of magnetic induction. Current I is pulsed through a stimulating coil with configuration s, creating an effective magnetic field at any point r. As this magnetic field changes in time, it induces an electric field

$$\vec{E}(\vec{r}) = -\frac{\partial I}{\partial t} \frac{\mu_0}{4\pi} \int_s \frac{d\vec{l}'}{|\vec{r} - \vec{r}'|^3} - \nabla\Phi. \tag{2}$$

where $d\vec{l}'$ is an infinitesimal coil section in configuration s, $\vec{r}'$ is the corresponding vector from each section to the point $\vec{r}$ and Φ is the electric potential arising from surface charge accumulating at interfaces between nonhomogenous conductors. Since our experiment was conducted in a plane that is parallel to the plane of the stimulating coil, surface charge terms on interfaces parallel to these planes can be neglected. Charge accumulation on the boundaries of our experimental dish cannot be neglected but we will reason shortly that their effect on stimulating the nerve is minor. A model of our experimental stimulation coil is described in Fig. 1. We used (2) to calculate the electric field induced by discharging a pulse of current I through a figure-eight double coil positioned 5 mm below the plane of interest. In our experiment, we discharged sinusoidal currents with a sine cycle

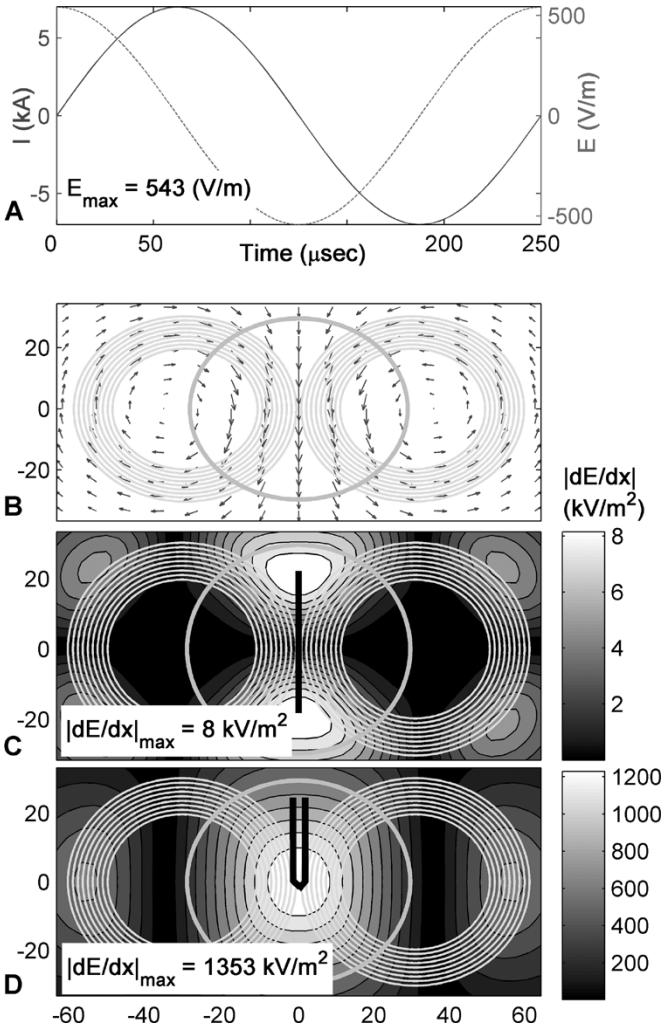

Fig. 1. Modeling the fields created by the coil configuration. (a) Time behavior of the maximum value of the electric field (dashed curve) induced by a discharge of current (solid curve) through the coils (time is measured from pulse initiation). (b) Two magnetic coils (9 windings in each coil) in a figure eight configuration carry opposite electric currents. (Right coil—in the clockwise direction and vice versa). Vector map indicates the maximum electric field induced by an abrupt discharge of current through the coils which are positioned 5 mm below the plane of the figure (electric field was calculated using (2) with the parameters listed in Table I). The central circle indicates the boundaries of the dish which was used in the experiment. (c) The maximal absolute value of electric field gradients along a straight nerve oriented parallel to the y axis. Each point in the figure indicates the electric field gradient that would have been induced if the nerve was positioned at that point. The central circle indicates the boundaries of the dish and the black line illustrates a straight nerve above the coil center. (d) The maximal absolute value of electric field gradients along a nerve which bends from the $-$y direction to $+$y direction in half a loop of radius 0.4 mm. Each point in the figure indicates the electric field gradient that would have been induced if the nerve bend was positioned at that point. The central circle indicates the boundaries of the dish and the black line illustrates a nerve bend over the center of the coil (not to scale). All distances are in units of the length constant λ.

of 250 μs. The time behavior of the discharged current and the induced electric field are illustrated in Fig. 1(a). The temporal pattern of the pulses remained constant throughout the experiment while their amplitude was repeatedly varied to determine threshold stimulation values. To simulate the stimulating coil in our experiment we used 9 concentric current loops for each side of the coil, and the vertical location of these two-dimensional loops was such that it maximized the similarity between

TABLE I
MODEL PARAMETERS. TIME AND LENGTH CONSTANTS ARE CALCULATED FROM [15] FOR THE RELEVANT AXON DIAMETER d_0

Symbol	Quantity	Value
I	The pulse of current discharged through the coils	$I = I_0 \sin\left(\frac{2\pi}{T}\cdot t\right)\ t = 0..T$
T	The duration of the pulse	$250\mu s$
I_0	The peak current of the pulse	$7kA$
s	Coil configuration	A pair of 9 concentric current loops 60-92mm in diameter positioned 94mm apart. The plane of the current loops was located at a vertical distance of 12mm from the outer surface of the coil housing.
Z	Vertical distance to outer surface of coil housing	$5mm$
d_0	Outer radius of axon	$13\mu m$
τ	Membrane time constant	$39\mu s$
λ	Membrane length constant	$1.5mm$
r_t	Radius of turn	$0.4mm$

the calculated magnetic field and the technical data sheet of the Double 70 mm coil by Magstim Company (Whitland, U.K). The exact modeling of the coil is described in Table I while Fig. 1(b) illustrates the coil configuration and the electric field it induces. The maximum value of the induced electric field is given in Fig. 1(a). This value denotes the predicted maximum of electric field induced by setting the TMS to 100% of its power. The absolute value in V/m of any threshold power (denoted in this paper by percentage of maximum stimulation) can be inferred by multiplying this absolute maximum value with the percentile threshold value.

To demonstrate the effect of curvature in our model, we compared the values of the electric field gradient along the nerve [$\partial E_x/\partial x$ from (1)] for two different nerve trajectories. Fig. 1(c) illustrates the calculated values for a straight nerve oriented parallel to the y axis of the figure while Fig. 1(d) illustrates the calculated values for a nerve which bends from the $-$y direction to $+$y direction in half a loop of radius 0.4 mm. Since the discharging pulses are bipolar, only absolute values of the field gradients were considered. From this comparison we notice that the effect of nerve curvature in the current experimental setup is more than 100 times stronger than the effect of electric field gradients produced by spatial configuration of the coils. This is because the curvature length scales are approximately 0.5 mm while the spatial configuration length scales are approximately 50 mm (similar to the dimensions of the coil). The straight nerve may also be excited, but this is due to the existence of nerve endings in it, which create a spatial inhomogeneity that contributes to the induced electric field approximately 50% of what half a loop contributes.

Since our experiment was conducted inside a finite dish, surface charge is expected to accumulate on the boundaries of this

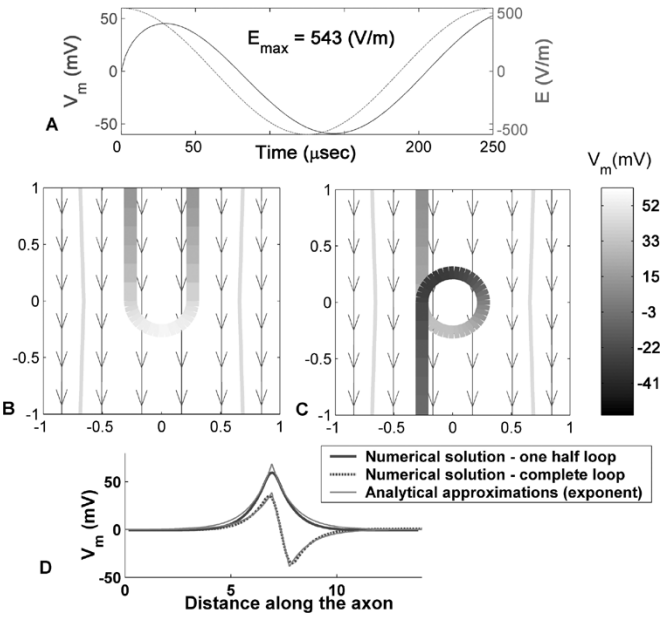

Fig. 2. (a) Maximum membrane potential (solid curve) and the electric field [dashed curve, see Fig. 1(a)] of a nerve bent over the coil center as in Fig. 2(b) (time is measured from pulse initiation). (b) Zooming in on the center of Fig. 1(b), the passive effect of the induced electric field (vector map) on an axon (thick curve) is numerically solved at the time of maximum induced field. The axon was curved to form half a loop of radius r_t around the origin. Gray levels on thick curve represent membrane potential numerically solved using (1) and (3) with the parameters listed in Table I. (c) Same as (b) with an axon curved to form a complete loop of radius r_t around the origin. d) the membrane potential along the two axons curved at either half (solid line) or complete (dashed line) loop at time of maximum induced field. Thin lines represent the analytical approximations (exponent) of the two configurations according to the Appendix. All distances are in units of the length constant λ. Notice the canceling effects in the complete loop curvature.

dish. However, the electric field arising from these charges can be shown to be no more than 20% of the magnetically induced electric field, while the spatial gradients are relatively small and typically set by the large scale of the sample boundaries. This electric field arises from charges outside the axon membrane, and does not affect the induced field inside the axon membrane directly. It is rather like electric stimulation with extra-cellular electrodes, but with electric field gradients which are over 100 times weaker than those inside the axon [see Fig. 1(c), (d)].

Since we only measure threshold values of curved nerves in our experiment, we restrict our model to deal only with uniform electric fields whose contribution to stimulation arises from their action on the curved nerve. The maximal gradient of electric field is obtained by positioning nerve bends in the center of the coil and the induced electric field in this region (a rectangle of 2×12 length constants around the center of the coils) does not deviate more than 5% from its value in the center. In such a case, the gradient of the electric field along the axon is affected only by the change of axon direction $\hat{x}$

$$\frac{\partial E_x}{\partial x} = E\frac{\partial(\hat{E}\cdot\hat{x})}{\partial x} = -E\sin\alpha\frac{\partial\alpha}{\partial x} \tag{3}$$

where $\hat{E}$ is a unit vector in the direction of the induced electric field and α is defined as the angle between the direction of the axon and the direction of the induced electric field. A model of a curved axon in a uniform electric field is described in Fig. 2. The figure-eight double coil is positioned 5 mm below the nerve. The gradient of the electric field along the axon $\partial E_x/\partial x$ was calculated with (3) and the resulting membrane potential was calculated with (1). Model parameters are listed in Table I.

Passive membrane dynamics tend to follow the stimulus pattern, with a delay that depends on the ratio between the stimulus time constant and the membrane time constant [Fig. 2(a)]. The spatial pattern of the membrane potential forms a sharp peak where the absolute value of $\partial E_x/\partial x$ is maximal, i.e., at the curved section whose tangent is perpendicular to the induced field. The amplitude of this peak scales with the length constant λ, as demonstrated in the Appendix. The effect of the magnetic field on the membrane potential of curved axons can be intuitively explained in the following way: the induced electric field [vector field in Fig. 2(b)] drives positively charged ions in the direction of the arrows. Such ionic currents coming from both sides of the axon curve accumulate at the lower part of the curve, creating a local excess of positive charges relative to the external medium and, therefore, a positive potential difference.

When the axon is curved into a complete loop [Fig. 2(c)], the same effect that created positive potential on the membrane in the lower part of the curve is now responsible for the negative potential on the membrane in the upper half of the loop. This creates a bipolar pattern of the potential, canceling some of the effect. The maximal potential in the complete loop configuration is, thus, attenuated compared to that in the half loop configuration [Fig. 2(d)].

Further simplifications provide an analytic description of the canceling effect. Assuming that the axon is curved into N half loops of radius r_t, the minimum electric field $E_{\min}$ which will trigger an action potential (henceforth, denoted "Threshold Power") can be approximated by

$$\frac{1}{E_{\min}} = \frac{A\lambda}{V_T}\int_{n=0}^{N-1}(-1)^n e^{-\frac{n\pi r_t}{\lambda}}. \tag{4}$$

with A a dimensionless fit parameter. Equation (4) is derived in the Appendix.

III. Methods

A. Nerve Dissection

Rana Ridibunda (Marsh Frog) was pithed and its spinal cord severed. The sciatic nerves were isolated and removed with the Gastrocnemius muscle intact. Proximal end of nerve was ligated. The nerve and muscle were immersed in Frog Ringer solution (NaCl 116 mM, KCl 2 mM, CaCl2 1.8 mM, HEPES 5 mM, Ph7.4 with NaOH). All experiments were approved by the Weizmann Institutional Animal Care and Use Committee (IACUC).

B. Magnetic Stimulator

We used the Magstim Rapid with 70-mm Double Coil. We checked that the stimulating pulse is a single sine cycle, 250 μs in duration with a peak discharge current of up to 7 kA [16]. These specifications match the stimulating parameters of the model as described in Fig. 2. The Output Control knob of the stimulator sets the peak discharge current to a required fraction of the maximal output of 7 kA with a resolution of $\pm 1\%$.

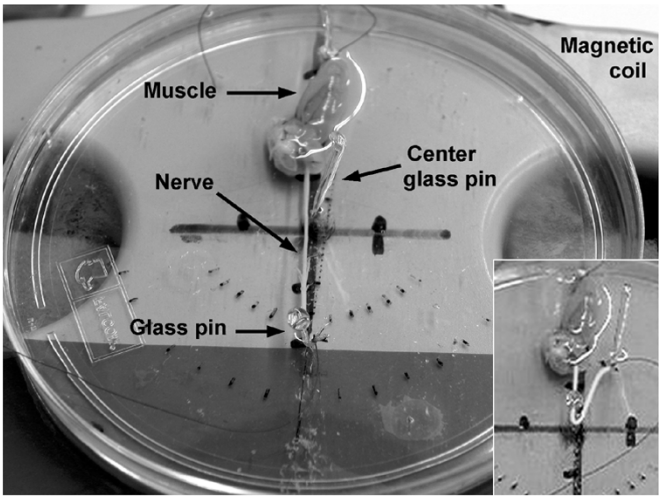

Fig. 3. Experimental setup. The double coil is placed below the plate, to which the nerve and muscle are fixed by glass pins. Inset shows a half loop configuration ($N = 1$) with the nerve wrapped around the center glass pin.

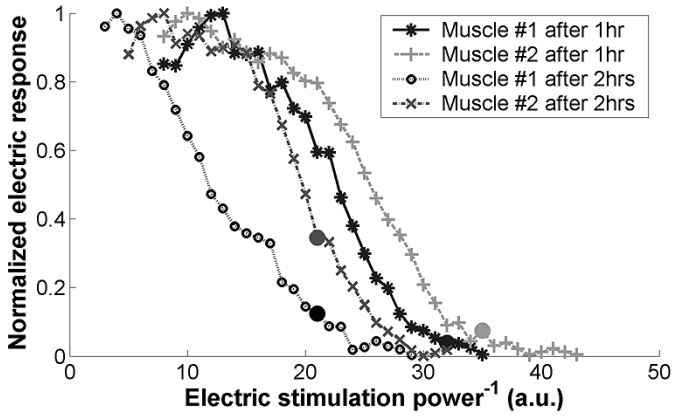

Fig. 4. Electric response of two nerve-muscle preparations was measured for decreasing stimulation power. Minimum power for which muscle twitching was still observable is indicated by filled circles. Each of the two preparations was measured 1 and 2 h after dissection.

C. Setup Configuration

The Stimulator coil was placed flat on a table, with the plate containing the nerve and muscle lying over it. The bottom of the plate was filled with an elastomer, resulting in a vertical separation of 4 mm between the nerve and the coil. Nerve and muscle were pinned to the elastomer floor with glass pins, immersed in Frog Ringer solution. The initial orientation of the nerve and muscle was aligned with the axis of the coil handle, i.e., the y-axis in the model section. Curving of the nerve bundle was achieved by wrapping the bundle around additional glass pins. The diameter of the glass pins was 0.5 mm and the winding of the pitch was approximately the diameter of the nerve (0.3 mm). The experimental setup is described in Fig. 3.

D. Measurements

The parameter measured in the experiments was the threshold power, i.e., the minimum Magstim power setting required in order to initiate an action potential in the nerve. This threshold was determined by the following protocol: First, Magstim power was increased rapidly until muscle twitching was clearly observed by eye. Then power was decreased in steps of 2%, until no twitching was observed. The Threshold Power was measured as the mean power percentage of the last two steps, i.e., 1% below the last power in which twitching was still observed. Measuring error was assumed to be $\pm 1\%$. To verify that muscle twitching is indeed a good indicator of nerve excitation, we measured in a separate experiment also the nerve's electrical response, and found that the threshold potential as determined visually coincides precisely with the one determined electrically. Electric recording was performed with an extra-cellular pipette filled with frog ringer solution, using an Axon AM 3000 (no filtering) at X100–X1000 amplification.

IV. Results

A. Simultaneous Measurement of Nerve Action Potentials and Muscle Twitching

To assure that the Threshold Power was correctly assigned a comparison was made between visual detection of the twitch of the muscle and measurements of electrical activity in the nerve. Nerves were excited with magnetic or electric stimulation while being electrically recorded. The minimum electric response for which muscle twitching could be observed was measured for two nerve-muscle preparations, at 1 hr after dissection and 2 h after dissection. Results are presented in Fig. 4. Muscle twitching was observed at a minimal electrical response of 4% and 7% of the maximum electric response 1 h after dissection. Some fatigue is noticeable for the measurements 2 h after dissection, where muscle twitching was observed at a minimal electrical response of 12% and 34% of the maximum electric response respectively.

B. Measuring Threshold Power in the Loops Configuration

Fourteen nerves were curved into integer number of half loops, from one half loop through single up to 3.5 loops. Nerve orientation was parallel to the y-axis (as in the model). Nerves were curved in either clockwise or anti-clockwise loops around a glass pin with a diameter of 0.5 mm. Threshold Power was measured for each configuration and then averaged and inverted to represent $1/E_{\min}$ as in (4) [Fig. 5(c)].

At this stage we are ready to extract the length constant, which is the relevant parameter for propagation of an action potential in the nerve. We first use these results to estimate the ratio between the length constant and the radius of curvature by plotting the absolute difference between Thresholds of consecutive N's. It can be shown that these differences decay exponentially (assuming $1/E_{\min}(0) = 0$)

$$\left| \frac{1}{E_{\min}(N+1)} - \frac{1}{E_{\min}(N)} \right| \sim e^{-\frac{N\pi r_t}{\lambda}}. \tag{5}$$

Fig. 6 fits the absolute difference between thresholds of consecutive Ns with an exponential fit to derive $\lambda/r_t = 3.8 \pm 0.35$. Plugging in the glass pin diameter of 0.5 mm and an average nerve bundle diameter of 0.3 mm we can estimate the turning radius to be $r_t = 0.25 + 0.15 \text{ mm} = 0.4 \text{ mm}$. After substituting we end up with $\lambda = 1.52 \pm 0.14 \text{ mm}$.

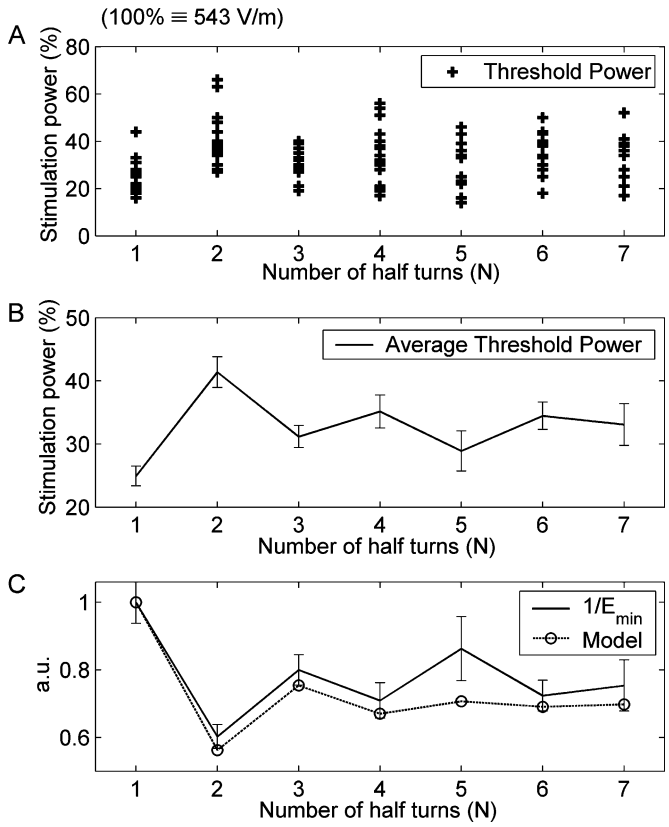

Fig. 5. (a) Threshold Power of 14 nerves was measured for curving of N half loops. (b) Average threshold power of (a). (c) Average threshold power of (a) inverted and normalized $(1/E_{\min})$. The dashed line is the prediction of (4).

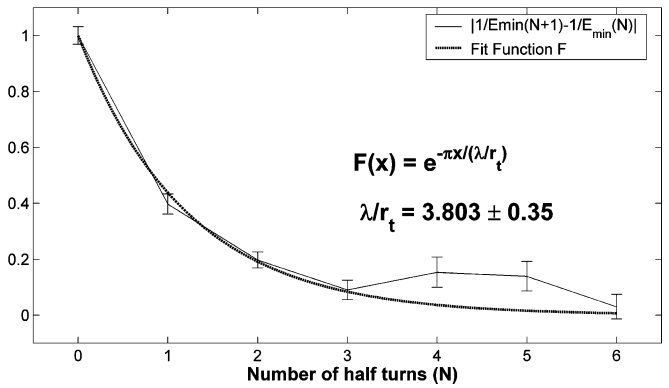

Fig. 6. Estimating λ/r_t. Absolute difference between thresholds of consecutive Ns is fitted by an exponential fit.

C. Measuring Threshold Power in an Elliptic Loop

An alternative configuration for measuring the length constant is by creating an ellipse. Four nerves were curved into a single loop with variable ellipticity, composed of two half turns made at a varying distance. Nerves orientation was parallel to the y-axis (as in the model). Nerves were curved in either clockwise or anti-clockwise loops around two glass pins each with a diameter of 0.5 mm. The y-distance r between the two glass pins was increased from 0 mm to 5 mm while the Threshold Power was measured for each distance.

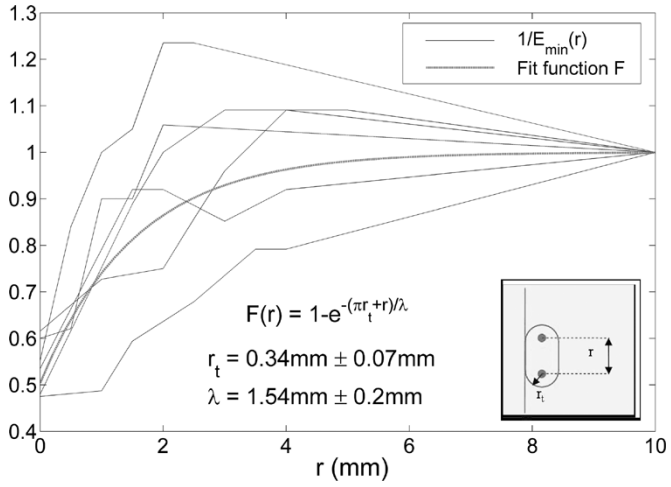

Fig. 7. Estimating λ and r_t. Inverted and normalized threshold versus r is fitted with the function $F(r)$ which is described in Section IV-C. Inset shows the elliptic loop configuration. Nerves were curved around two glass pins. The y-distance between the two pins (r) was varied during the experiment.

The inverted Threshold Power for an axon curved into two half loops of radius r_t separated by a distance r can be approximated by (taking the same considerations described in the Appendix)

$$F(r) = 1 - e^{-\frac{\pi r_t + r}{\lambda}}. \tag{6}$$

In Fig. 7, the threshold power is inverted and normalized (according to $1/E_{\min}(r) \underset{r\to\infty}{=} 1$). The fit of $1/E_{\min}(r)$ according to the configuration function $F(r)$ is displayed. From this fit, the length constant and curve radius can be estimated independently: $\lambda = 1.54 \pm 0.20$ mm and $r_t = 0.34$ mm ± 0.07 mm. These results are consistent with those derived with the previous method in Section IV-B.

Using this, we can obtain theoretical values for the diameter of the single nerves in the bundle. The theoretical relation between the length constant and the diameter of myelinated axons can be calculated using accepted values for resistivity of the axoplasm and myelin and conductivity of nodes of ranvier [15], [17]: $\lambda = 117\,\mathrm{d}$. The axon diameter that matches our measured length constant is $d = 13\ \mu$m.

V. Conclusion

In this paper, we have demonstrated how measurements of magnetic stimulation thresholds (the power threshold) can have qualitative as well as quantitative capabilities in exploring the passive properties of nerves. The effect of axonal curvature on magnetic stimulation of peripheral nerves is well described by passive membrane models of the axon. The measured voltage length constant is consistent with the range of measured values in the literature [18].

Numerical simulations show that the electric field gradient that is created by nerve curvature of the scale used in our experiment (or of nerve endings) is more than 100 times greater than the electric field gradient created by the coil configuration used in our experiment. Since 20% of the maximal TMS power

is still needed to stimulate curved nerves, while the spatial gradients of the TMS coil are 100 times weaker, we can deduce that TMS can excite a nerve only if it has endings or curvature (even small undulations suffice [19]).

The Power Threshold method improves and expands other electrophysiological methods that were used to explore the effects of magnetic stimulation on nerves [20], and was proven in this experiment to be both simple and reliable. Its simplicity emerges both from the noninvasive and straightforward measurements and from the fact that it is independent of the active properties of the nerve. By using minimal power to stimulate the nerve we probe its passive properties only and elicit a consistent and reliable response from the biological preparation.

As for the length constant of nerve, till now it could only be obtained using electrophysiological methods. An indirect estimation of the length constant was obtained by recording from a single electrode [21], [22], while a direct measurement of the length constant required more complicated methods such as voltage sensitive dyes [23] or multi-electrode recording [24]. *In vitro*, the power threshold method may be modified and used for any magnetically stimulated nerve with known geometry, thus enabling a simple and direct method of measuring the length constant. Applying it on humans may be possible wherever adequate control of nerve curvatures can be achieved. Furthermore, passive time constants can be derived by determining the threshold power of two consecutive pulses with a given time difference. Similarly to the two-bends experiment (Fig. 7), the threshold will also depend exponentially on the time difference, with the passive time constant in the exponent. Plotting threshold as a function of the time differences, we would fit the behavior with a function that depends on the passive time constant of the axon.[1]

In the future, applying the method we have presented here on increasingly complex neural networks (neural cultures, slices and living brains) will help us predict and understand better the interaction of the stimulation with curved neural substrate, and possibly improve our ability to affect activity in the cortex of humans.

APPENDIX

The canceling effect of multiple loops in a single axon can be investigated using the following simplifications. Considering the magnetic stimulation at the moment of maximal membrane potential, we can neglect the time dependence of (1)

$$\lambda^2 \frac{\partial^2 V_m}{\partial x^2} - V_m = \lambda^2 \frac{\partial E_x}{\partial x}. \tag{7}$$

To approximate the induced electric field in one half loop configuration we use (3) and replace the sine function with one sharp peak

$$\frac{\partial E_x}{\partial x} = -E\frac{\partial \alpha}{\partial x}\sin\alpha = -E\frac{1}{r_t}\sin\frac{x}{r_t} \underset{r_t\to 0}{\longrightarrow} -2E\cdot\delta(x). \tag{8}$$

E is the amplitude of the induced electric field as described in Fig. 1 and $\delta(x)$ is Dirac's delta function. This approximation is valid assuming zero gradient of electric field except at the region of the curve and a radius of curvature which is small enough (compared to λ). The solution of (7) with such an external term will be

$$V_m = A\cdot\lambda\cdot E\cdot e^{-\frac{|x|}{\lambda}}. \tag{9}$$

A is a dimensionless coefficient which takes into account the temporal effects of the external field on the amplitude of the membrane potential. For configurations of more than one half loop, a superposition of such terms is suggested. Each term is opposite in sign compared to its neighboring terms (since the direction of the induced electric field with respect to the direction of the nerve is opposite) and is separated from its neighboring by the distance of one half loop along the axon (which can be expressed as πr_t). Therefore the membrane potential of a configuration of N half loops can be expressed as

$$V_m = A\cdot\lambda\cdot E\cdot\sum_{n=0}^{N-1}(-1)^n e^{-\frac{|x-n\pi r_t|}{\lambda}}. \tag{10}$$

In our experiment, we measure the minimum value of the stimulation power $E_{\min}$ (denoted as the Threshold Power) required to initiate an action potential in nerves of different configuration. This is the power which creates the minimal membrane potential required for initiating an action potential, i.e., V_T (denoted as the threshold potential). This potential threshold is not constrained to a specific location on the axon; therefore, we can define the threshold equation as

$$V_T = A\cdot\lambda\cdot E_{\min}\cdot\max_x\left\{\sum_{n=0}^{N-1}(-1)^n e^{-\frac{|x-n\pi r_t|}{\lambda}}\right\}. \tag{11}$$

For a nerve curved to form a given number N of half loops we define the configuration function $f_N(x)$ as

$$f_N(x) = \sum_{n=0}^{N-1}(-1)^n e^{-\left|\frac{x-n\pi r_t}{\lambda}\right|}. \tag{12}$$

Thus, for a given number of half curves N

$$\frac{1}{E_{\min}} = \frac{A\lambda}{V_T}\max_x\{f_N(x)\}. \tag{13}$$

To predict the Threshold Power of each configuration, one must find the maximum value of the configuration function $f_N(x)$. It can be shown that the maximum value of a sum of opposing exponents is obtained at the extreme peaks of the sum

$$\max_x\{f_N(x)\} = f_N(0) = \int_{n=0}^{N-1}(-1)^n e^{-\frac{n\pi r_t}{\lambda}}. \tag{14}$$

Finally, combining the last two equations, one gets (4)

$$\frac{1}{E_{\min}} = \frac{A\lambda}{V_T}\int_{n=0}^{N-1}(-1)^n e^{\frac{-n\pi r_t}{\lambda}}.$$

ACKNOWLEDGMENT

The authors would like to thank I. Fishbein, G. Glusman, A. Pressman, and R. Tal for technical assistance, and E. Alvarez Lacalle, R. Bistricher, D. Biron, I. Breskin, O. Feinerman, S. Jacobi, N. Levit Binnun, and T. Tlusty for helpful discussions.

[1]The preferred stimulation waveform for this measurement would be a monopolar pulse with a time constant shorter than the passive time constant.

REFERENCES

[1] A. T. Barker, R. Jalinous, and I. L. Freeston, "Non-invasive magnetic stimulation of human motor cortex," *Lancet*, vol. 1, no. 8437, pp. 1106–1107, May 1985.

[2] M. S. George, E. M. Wassermann, and R. M. Post, "Transcranial magnetic stimulation: a neuropsychiatric tool for the 21st century," *J. Neuropsych. Clin. Neurosci.*, vol. 8, no. 4, pp. 373–382, Fall 1996.

[3] M. Hallett, "Transcranial magnetic stimulation and the human brain," *Nature*, vol. 406, pp. 147–150, Jul. 2000.

[4] A. Pascual-Leone *et al.*, *Handbook of Transcranial Magnetic Stimulation*. London, U.K.: Arnold, 2002.

[5] S. Pridmore, "Substitution of rapid transcranial magnetic stimulation treatments for electroconvulsive therapy treatments in a course of electroconvulsive therapy," *Depression Anxiety*, vol. 12, no. 3, pp. 118–123, Nov. 2000.

[6] A. Post and M. E. Keck, "Transcranial magnetic stimulation as a therapeutic tool in psychiatry: what do we know about the neurobiological mechanisms?," *J. Psych. Res.*, vol. 35, pp. 193–215, 2001.

[7] M. Kobayashi and A. Pascual-Leone, "Transcranial magnetic stimulation in neurology," *Lancet Neurol.*, vol. 2, no. 3, pp. 145–156, Mar. 2003.

[8] J. P. Brasil-Neto, L. G. Cohen, M. Panizza, J. Nilsson, B. J. Roth, and M. Hallett, "Optimal focal transcranial magnetic activation of the human motor cortex: effects of coil orientation, shape of the induced current pulse, and stimulus intensity," *J. Clin. Neurophysiol.*, vol. 9, no. 1, pp. 132–136, Jan. 1992.

[9] K. R. Mills, S. J. Boniface, and M. Schubert, "Magnetic brain stimulation with a double coil: the importance of coil orientation," *Electroencephalogr. Clin. Neurophysiol.*, vol. 85, no. 1, pp. 17–21, Feb. 1992.

[10] A. Pascual-Leone, L. G. Cohen, J. P. Brasil-Neto, and M. Hallett, "Non-invasive differentiation of motor cortical representation of hand muscles by mapping of optimal current directions," *Electroencephalogr. Clin. Neurophysiol.*, vol. 93, no. 1, pp. 42–48, Feb. 1994.

[11] A. G. Guggisberg, P. Dubach, C. W. Hess, C. Wüthrich, and J. Mathis, "Motor evoked potentials from masseter muscle induced by transcranial magnetic stimulation of the pyramidal tract: the importance of coil orientation," *Clin. Neurophysiol.*, vol. 112, no. 12, pp. 2312–2319, Dec. 2001.

[12] P. Dubach, A. G. Guggisberg, K. M. Rösler, C. W. Hess, and J. Mathis, "Significance of coil orientation for motor evoked potentials from nasalis muscle elicited by transcranial magnetic stimulation," *Clin. Neurophysiol.*, vol. 115, no. 4, pp. 862–870, Apr. 2004.

[13] K. J. Smith and W. I. McDonald, "The pathophysiology of multiple sclerosis: the mechanisms underlying the production of symptoms and the natural history of the disease," *Philos. Trans. Roy. Soc. Lond., B—Biol Sci*, vol. 354, no. 1390, pp. 1649–1673, Oct. 1999.

[14] B. J. Roth and P. J. Basser, "A model of the stimulation of a nerve fiber by electromagnetic induction," *IEEE Trans. Biomed. Eng.*, vol. 37, no. 6, pp. 588–597, Jun. 1990.

[15] P. J. Basser and B. J. Roth, "Stimulation of a myelinated nerve axon by electromagnetic induction," *Med. Biol. Eng. Comput.*, vol. 29, no. 3, pp. 261–268, May 1991.

[16] *Magstim Rapid Operating Manual*, Magstim Co., Whitland, U.K., 2002.

[17] R. B. Stein, *Nerve and Muscle: Membranes, Cells and Systems*. New York: Plenum, 1980.

[18] B. Katz, *Nerve, Muscle, and Synapse*. New York: McGraw-Hill, 1966.

[19] V. Schnabel and J. J. Struijk, "Magnetic and electrical stimulation of undulating nerve fibers: a simulation study," *Med. Biol. Eng. Comput.*, vol. 37, pp. 704–709, Nov. 1999.

[20] P. J. Maccabee, V. E. Amassian, L. P. Eberleand, and R. Q. Cracco, "Magnetic coil stimulation of straight and bent amphibian and mammalian peripheral nerve *in vitro*: locus of excitation," *J. Physiol.*, vol. 460, pp. 201–219, 1993a.

[21] J. K. Engelhardt, F. R. Morales, J. Yamuy, and M. H. Chase, "Cable properties of spinal cord motoneurons in adult and aged cats," *J. Neurophysiol.*, vol. 61, pp. 194–201, Jan. 1989.

[22] D. A. Turner and P. A. Schwartzkroin, "Electrical characteristics of dendrites and dendritic spines in intracellularly stained CA3 and dentate hippocampal neurons," *J. Neurosci.*, vol. 3, pp. 2381–2394, Nov. 1983.

[23] T. Berger, M. E. Larkum, and H.-R. Lüscher, "High Ih channel density in the distal apical dendrite of layer V pyramidal cells increases bidirectional attenuation of EPSPs," *J. Neurophysiol.*, vol. 85, pp. 855–868, Feb. 2001.

[24] A. A. Prinz and P. Fromherz, "Effect of neuritic cables on conductance estimates for remote electrical synapses," *J. Neurophysiol.*, vol. 89, pp. 2215–2224, Apr. 2003.

A. Rotem was born in Israel in 1972. He received the B.Sc. degree in physics and computer science from Tel-Aviv University, Tel-Aviv, Israel, in 2000 and the M.Sc. degree in physics from the Weizmann Institute of Science, Rehovot, Israel, in 2003. He is currently working toward the Ph.D. degree in the department of Physics of Complex Systems, Weizmann Institute of Science.

His research focuses on the mechanisms of transcranial magnetic stimulation.

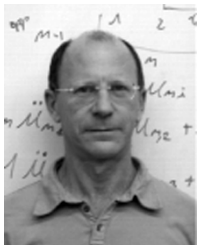

E. Moses was born in the United States in 1956. He received the B.Sc. degree in physics from the Hebrew University, Jerusalem, Israel, in 1981 and the M.Sc. and Ph.D. degrees in physics from the Weizmann Institute of Science, Rehovot, Israel, in 1983 and 1988, respectively.

He is currently a Professor in the Department of Physics of Complex Systems, Weizmann Institute of Science. His research is focused on understanding brain and neural activity.